# Quaternary, structural and engineering geology of the Aishihik River landslide, Cracker Creek area (NTS 115A/15), Yukon

***Marc-André Brideau[1]***
*Department of Earth Sciences, Simon Fraser University*

***Doug Stead***
*Department of Earth Sciences, Simon Fraser University*

***Crystal Huscroft***
*Department of Geography, University College of the Cariboo*

***Karin Fecova***
*Department of Earth Sciences, Simon Fraser University*

Brideau, M.-A. et al., 2005. Quaternary, structural and engineering geology of the Aishihik River landslide, Cracker Creek area (NTS 115A/15), Yukon. *In:* Yukon Exploration and Geology 2004, D.S. Emond, L.L. Lewis and G.D. Bradshaw (eds.), Yukon Geological Survey, p. 83-94.

## ABSTRACT

The Aishihik River landslide is a prehistoric slope failure located on a southwest-facing slope of the Ruby Range along the Alaska Highway. The failed mass consists of gneissic material from the Kluane metamorphic assemblage. Shoreline sediments from glacial lake Champagne were deposited on top of the landslide debris, suggesting that the slope failure occurred after the ice retreat but before the Dezadeash valley drained. Three dominant discontinuity sets were recognized and correlated to the fracturing associated with the formation of the Ruby Range antiform. Rock engineering classification and laboratory tests suggest that the rock mass present in the headscarp of the failure is of lower quality than on its sidescarps. This rock mass degradation was attributed to two intersecting fault sets at the headscarp. Tension cracks and trenches are present on all sides of the slope failure. Exposed soil and disturbed vegetation observed in trenches suggest continued instability.

## RÉSUMÉ

Le glissement de terrain de la rivière Aishihik s'est produit à la préhistoire sur une pente de la chaîne Ruby faisant face au sud-ouest, le long de la route de l'Alaska. La masse effondrée est formée de matériau gneissique de l'assemblage métamorphique de Kluane. Des sédiments littoraux du lac glaciaire Champagne se sont déposés sur les débris du glissement de terrain, ce qui porte à croire que ce dernier s'est produit après la récession glaciaire mais avant que la vallée de la Dezadeash ne se draine. Trois ensembles de discontinuités dominants ont été relevés et corrélés aux fractures associées à la formation de l'antiforme de Ruby Range. La classification de la mécanique des roches et des essais en laboratoire portent à croire que la masse de roches présente dans l'escarpement à la tête du glissement est de moins bonne qualité que les roches dans les escarpements sur les côtés du glissement. Cette dégradation de la masse de roches est attribuée à deux séries de failles croisées à l'escarpement de tête. Des fissures et fossés de tension sont présents sur tous les côtés du glissement. Le sol exposé et la végétation perturbée qui ont été observés dans les fossés semblent indiquer que l'instabilité se poursuit.

[1]*Department of Earth Sciences, Simon Fraser University, 8888 University Drive, Burnaby, British Columbia, Canada, V5A 1S6, mbrideau@sfu.ca*

## INTRODUCTION

The Aishihik River landslide is a large prehistoric slope failure that occurred on a southwest-facing slope of the Ruby Range near the intersection of the Aishihik Road and the Alaska Highway (Fig. 1). The landslide was originally mapped as alpine moraines by Kindle (1952), and was only recently analysed as a slope failure (Huscroft et al., 2004; Fig. 2). Its volume has been estimated at 22 million m$^3$. The debris deposit consists predominantly of large subangular boulders (Huscroft et al., 2004). Examples from southern British Columbia have demonstrated that sites of prehistoric slope failures can be catastrophically reactivated (e.g., Mathews and McTaggart, 1969; Couture and Evans, 2000), and emphasize the importance of understanding their failure mechanisms and evaluating their present day stability. The fieldwork performed for this study combined elements of structural and engineering geology mapping. A total of 11 ground traverses were conducted and 1000 structural measurements were taken. GIS software was used to store, manage and display the field data. The role of each of the discontinuity sets on slope stability and failure mechanisms were investigated. This study is part of a larger project initiated to investigate the influence of tectonic structures, such as faults, shear zones and folds, on the quality of a rock mass and their effect on the stability of rock slopes.

## BEDROCK GEOLOGY

The Aishihik River landslide occurred in Mesozoic gneissic rocks that are part of the newly proposed Kluane metamorphic assemblage (KMA; Mezger 1997, 2000, 2003). Petrography of the gneissic rocks at the Aishihik River landslide revealed that major phases (>5%) are plagioclase, quartz and biotite, and minor phases (<5%) are chlorite, potassium feldspar, unidentified opaque minerals and zircon. These results correlate with the petrology reported by Mezger (1997) for the KMA. The dominant structural feature in the KMA is a pervasive foliation that dips to the northeast. The Aishihik River landslide occurred near the contact between the Ruby Range Batholith (RRB) and the KMA. The Ruby Range Batholith is a 200-km-long northwest-trending Eocene granodiorite (Muller, 1967). The contact between the KMA and RBB was not observed directly at the study area. Intermediate dykes and sills are more prevalent in

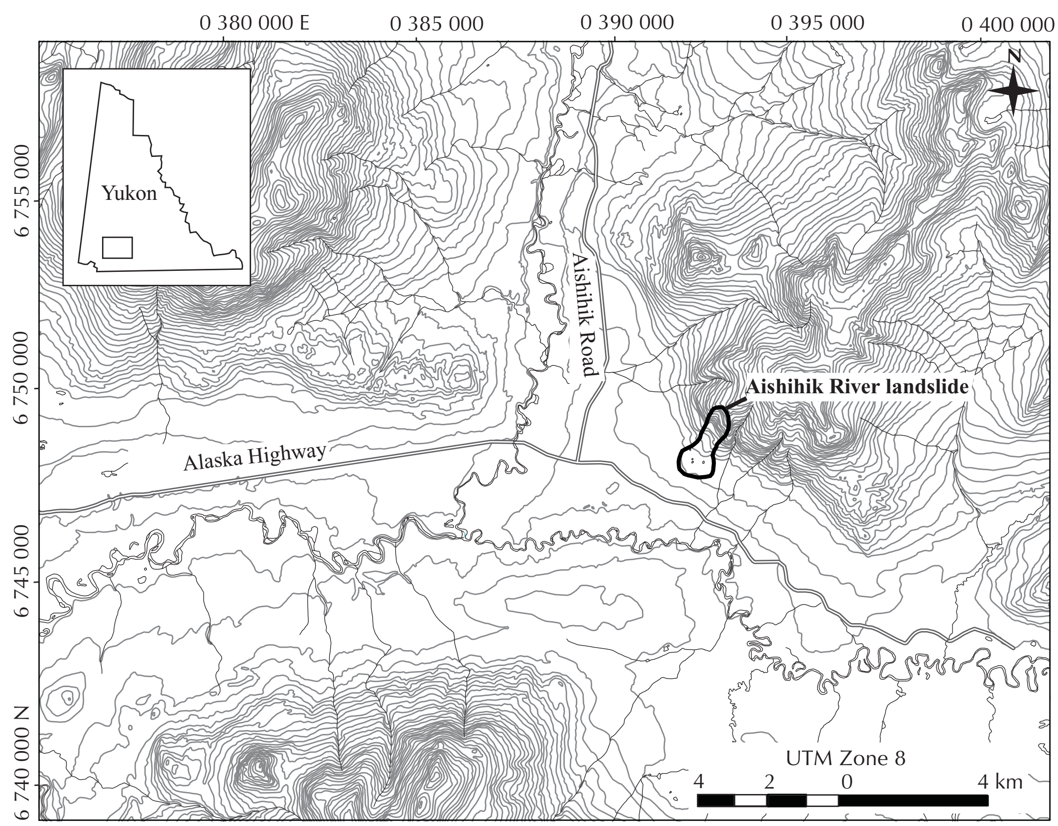


***Figure 1.*** *Location map of the Aishihik River landslide.*

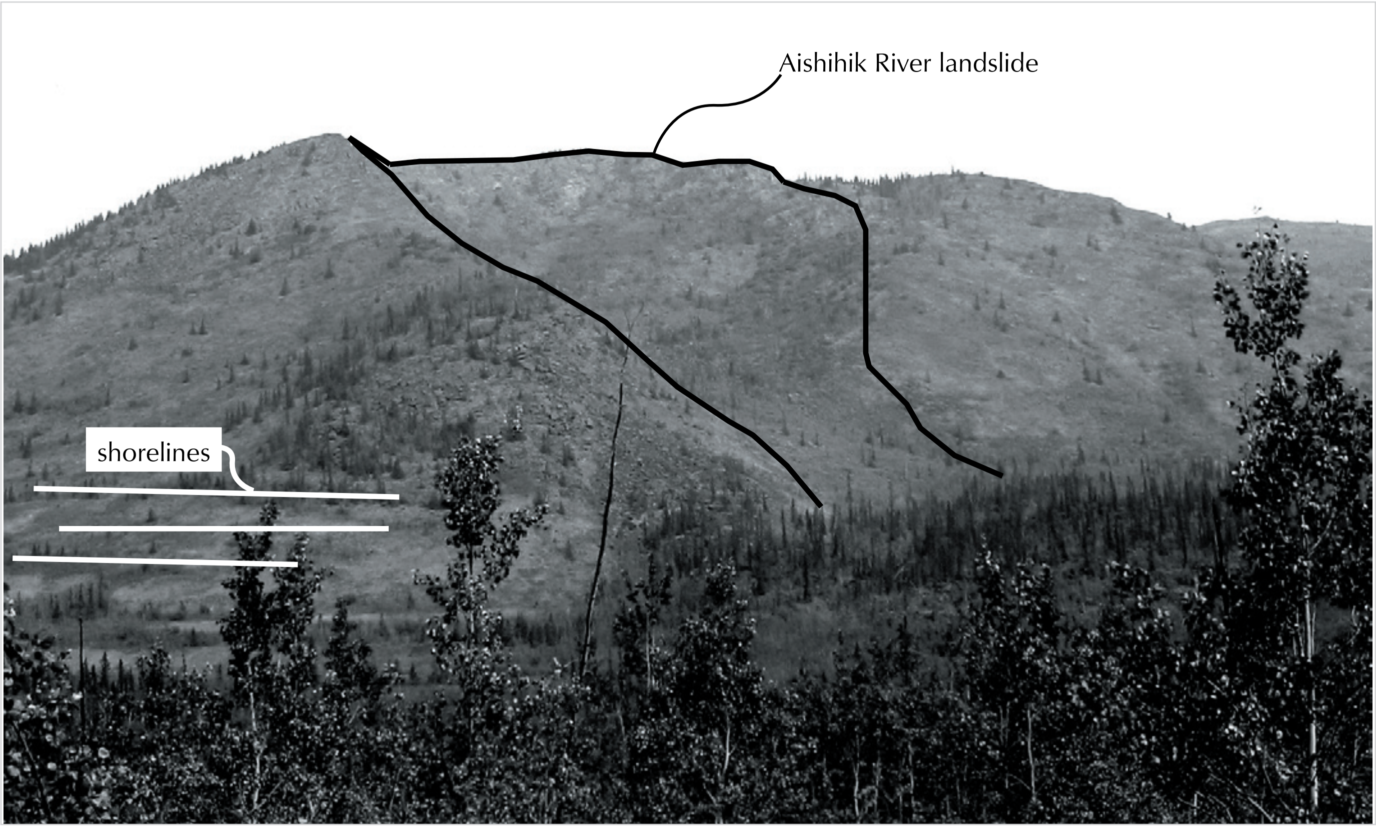


***Figure 2.*** *Overview of the Aishihik River landslide. View looking north.*

the northeastern section of the slope failure, and this increase in minor intrusive bodies is likely related to the proximity of the contact between the KMA and RBB. Contact metamorphism related to the intrusion of the RRB caused the predominantly schistose rocks of the KMA to be metamorphosed into gneissic rocks (Mezger, 1997, 2000).

## QUATERNARY GEOLOGY

The study area was last glaciated during the late Wisconsinan McConnell glaciation. At that time, ice in southwestern Yukon generally flowed out of ice centres in the most mountainous regions, such as the St. Elias and Coast Mountain belts, and along major structural trenches. Locally, ice flowed to the north across the Dezadeash River valley and up the Aishihik River valley (Hughes et al., 1989).

Glacial recession had initiated by 13 660 ± 460 years BP and occurred in a series of intervals of retreat and stagnation, with ice lobes occupying valley bottoms and damming numerous drainage routes (Hughes et al., 1989). Large glacial lakes were impounded in most of the main valleys, and included the Dezadeash and Aishihik river valleys. The intervals of stagnation resulted in the deposition of extensive glaciolacustrine deposits in valley bottoms and the formation of shoreline features on valley sides. Glacial lake shorelines eroded into the debris of the Ashihik River landslide are traceable between 810 and 850 m in elevation (Fig. 2). This lake level correlates with the earliest stages of the formation of glacial lake Champagne (Rampton and Paradis, 1982; Barnes, 1997; Barnes, 2000). Glacial lake Champagne was dammed by glacial ice and likely existed at its largest extent some time between 13 660 and 9500 BP (Hughes et al., 1989; Barnes, 1997).

## STRUCTURAL GEOLOGY

### DISCONTINUITY SETS AND STRUCTURAL DOMAINS

Three dominant discontinuity sets are prevalent over much of the study area (Fig. 3). The spacing and persistence categories proposed by the International Society for Rock Mechanics (ISRM1978) are employed in this paper. The first discontinuity set (I) trends west-northwest to northwest and dips subvertically. The second discontinuity set (II) trends northeast and also dips subvertically. Discontinuity sets I and II are nearly perpendicular to each other. Discontinuity set III trends north-northeast to northeast and dips at ~30°. Discontinuity set III is sub-parallel to the gneissic fabric. Three joint sets with similar orientations and spacings of less than 1 m were reported by Mezger (1997) for an area 20 km northwest of the Aishihik River landslide. Discontinuity set IV trends northwest and dips subvertically to the northeast. There is also a subordinate joint set that is not highlighted in the stereonets, since its spacing is wider than the area usually investigated at individual field stations. This joint set trends northeast and dips (40-50°) southeast, has a high strike and dip persistence (10 to 20 m), and an extremely wide spacing (>6 m).

The area of the Aishihik River landslide is divided into nine structural domains (Fig. 3A-I). The three discontinuity sets discussed above are present in domains A to E but have different orientations in each. These minor differences in orientation in domains A to E illustrate that the western sidescarp of the slope failure comprises a series of down-dropped blocks. Domain G, which encompasses the headscarp, is the only domain with a markedly different discontinuity pattern. The fault-parallel discontinuities related to the three northeast-trending minor faults mapped in the headscarp areas are part of discontinuity set II. A closely spaced joint set parallel to the headscarp was noted in the field and corresponds to discontinuity set IV in domain G. Discontinuity set IV is interpreted to be the field expression of a regional fault with a similar attitude (Fig. 4). Domain H on the eastern sidescarp of the slope failure is similar to domains A to E on the western sidescarp. Domains F and I have twice the number of discontinuity sets as the other domains. This is likely because the relatively few stations in these domains are located on blocks that have moved relative to one another. The spacing of the discontinuities is larger on the sidescarps (domains A to E, I, and part of H) than on the headscarp region (domain F, G, and part of H; Fig. 5). This

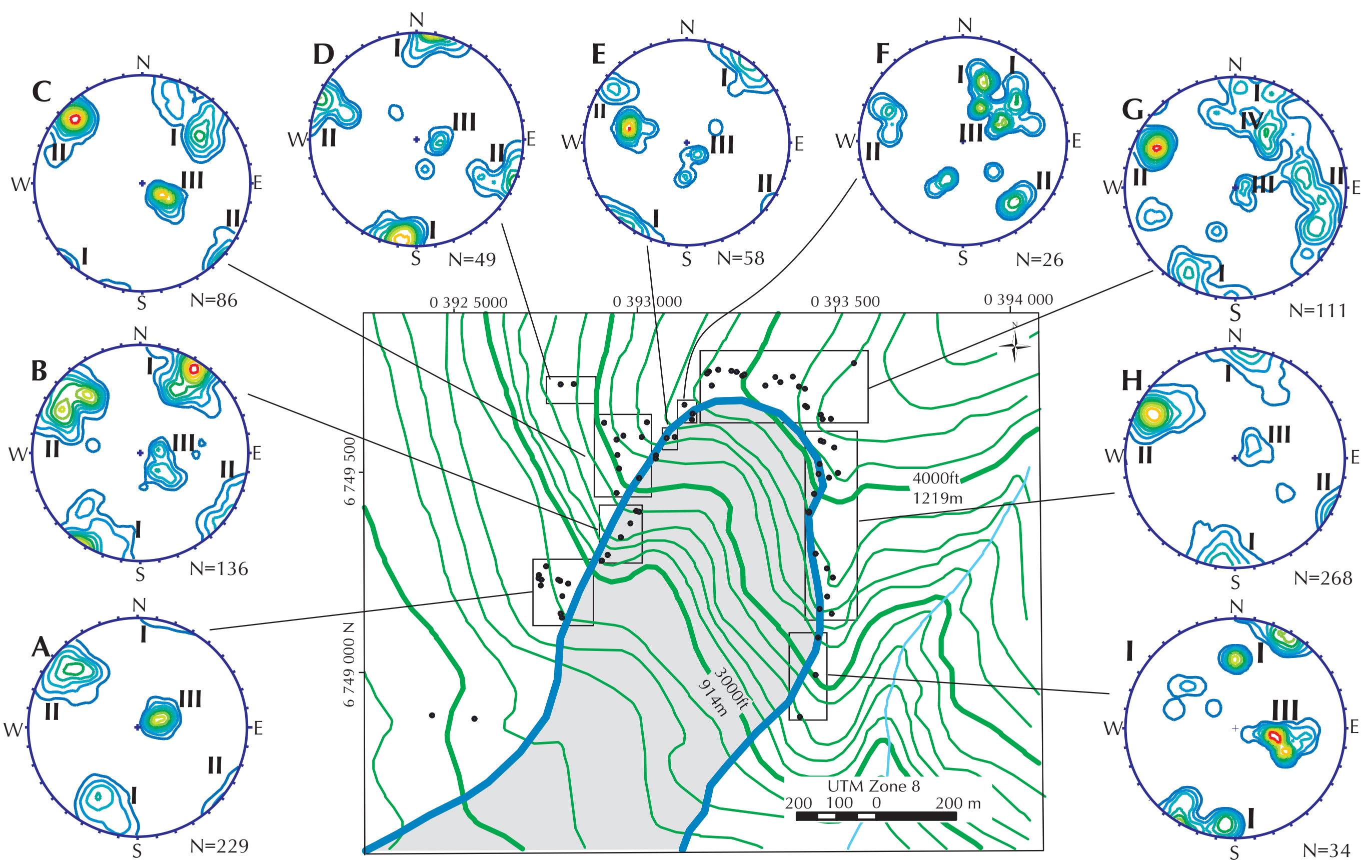


*Figure 3. Structural domains and accompanying contour plots of poles to the discontinuities. Stereonets are lower hemisphere Schmidt nets.*


***Figure 4.*** *Dominant discontinuity set IV in the headscarp area of the Aishihik River landslide. Note the close spacing (60 to 200 mm) of the discontinuity set.*

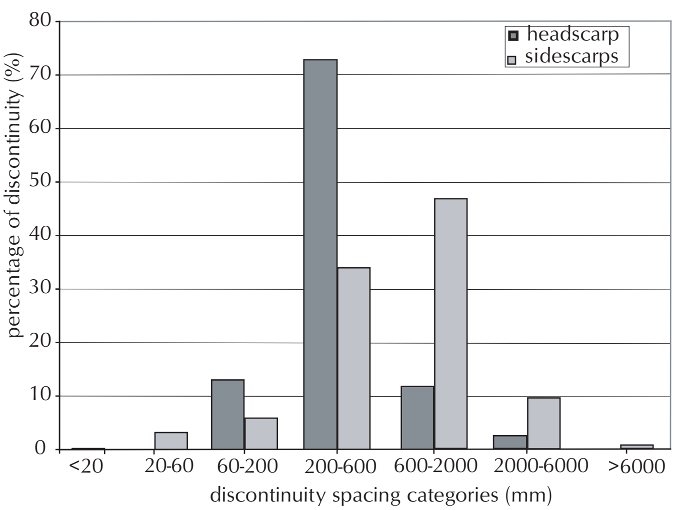


***Figure 5.*** *Percentage of discontinuity spacing categories at the Aishihik River landslide along the sidescarps and headscarp.*

correlates with the lower rock mass quality in the headscarp area (Fig. 4).

## FOLDING

The presence of a 20-km-wide antiform, termed the Ruby Range antiform, with its fold axis trending east-southeast in the McKinley River valley was proposed by Mezger (1997). The average gneissic mineral foliation measured at the study site strikes north-northwest and dips east-northeast at ~30°. This mineral foliation attitude indicates

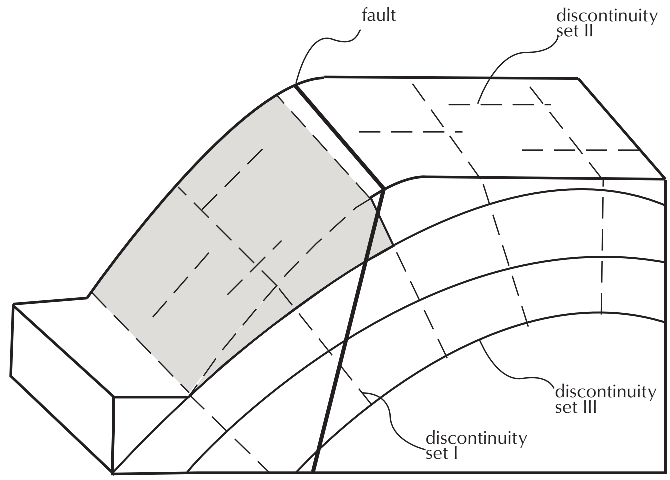


***Figure 6.*** *Geometry of fold, fault, discontinuities and slope at the Aishihik River landslide. The shaded area represents the unstable section of the slope.*

that the Aishihik River landslide is located on the southwestern limb of the Ruby Range antiform. The discontinuity sets present at the Aishihik River landslide can be related to simple fracturing models related to folding (e.g., Price and Cosgrove, 1990; Twiss and Moore, 1992; Davis and Reynolds, 1996; Fig. 6). Discontinuity set I consists of tensile fractures parallel to the fold axis, while discontinuity set II consists of tensile fractures perpendicular to the fold axis. Discontinuity set III consists of shear fractures that formed preferentially along pre-existing foliation planes during flexural folding.

## TENSION CRACKS AND TRENCHES

Twenty-five tension cracks and trenches were observed and described. Linear depressions clearly bounded by discontinuity sets are referred to as tension cracks whereas unbounded linear depressions in the landscape or soil cover are referred to as trenches. The tension cracks are concentrated on the western sidescarp of the slope failure, and are 2.5 to 30 m long and 0.5 to 14 m deep (Fig. 7). The trenches are concentrated behind the headscarp and along the eastern sidescarp, and are 5 to 150 m long and 0.3 to 5 m deep (Fig. 7).

The trenches behind the headscarp of the landslide exposed a thin (~20 cm) soil profile, which contained a discontinuous 2- to 5-cm-thick tephra layer 10 cm from the present day surface. The tephra layer likely represents deposits of the eastern lobe of the White River Ash (Lerbekmo and Campbell, 1969; Clague et al., 1995). The

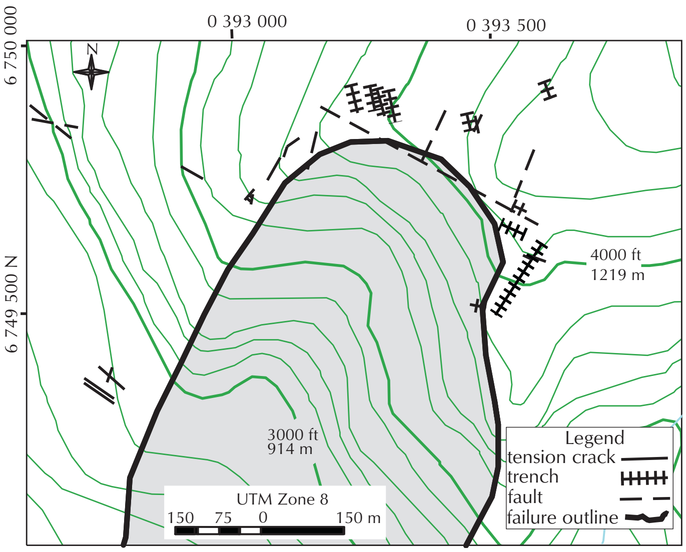


***Figure 7.*** *Location and orientation of faults, tension cracks and trenches described at the Aishihik River landslide.*

latest age constraints on the eastern lobe suggest deposition ~1150 years BP (Clague et al., 1995).

Two movement directions of slope material are highlighted by the tension cracks and trenches (Fig. 7). A first group of north-northwest trending tension cracks and trenches indicate a down-valley movement of material due to gravity. This group contains the trenches where soil and tephra are exposed. The second group of northeast-trending tension cracks and trenches reflects the dilational movement of the rock mass material associated with loss of restraint due to the prehistoric slope failure. Mature living trees were observed within some features of this group.

## FAULTS AND BEDROCK LINEAMENTS

Previously mapped faults (Gordey and Makepeace, 2000) within a 10-km radius of the Aishihik River landslide were compiled together with bedrock lineaments identified from air photographs (National Air Photo Library A25275-13,14; A31724-89,90) in a review of regional structures. Rose diagrams that illustrate the orientations of discontinuities, tension cracks and trenches, faults and bedrock lineaments are presented in Figure 8. All three types of structures have a well defined northeast trend concentration. The slope failure and runout direction also follow a northeast direction. Three minor faults with a northwest orientation were recorded at the headscarp of the Aishihik River landslide (Fig. 7). Timing constraints regarding the formation of the three types of structures

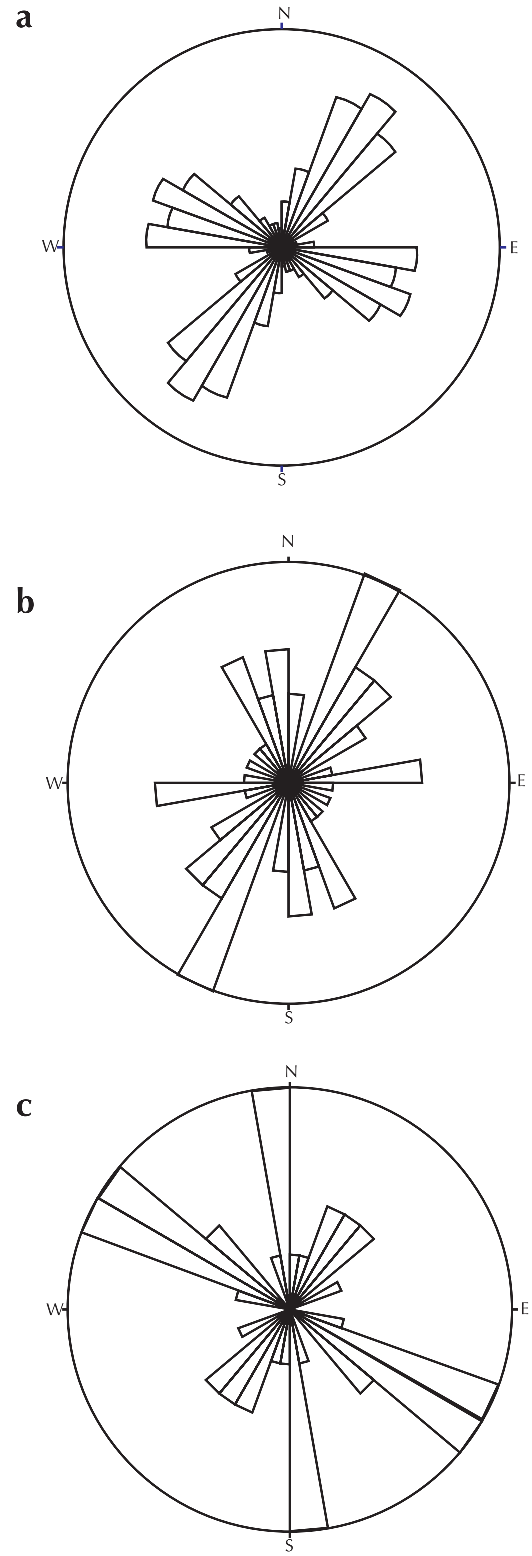


***Figure 8.*** *Symmetric rose diagrams comparing the orientation of discontinuities, faults and tension cracks.* ***(a)*** *discontinuities,* ***(b)*** *faults and bedrock lineaments,* ***(c)*** *tension cracks and trenches.*

were not evaluated at the Aishihik River landslide. A second west-northwest structural trend is dominant in the discontinuities and is present to a lesser extent in the faults and bedrock lineaments. This trend corresponds to the orientation of the headscarp. A third north-northwest structural trend was only present in the faults/bedrock lineaments and tension cracks/trenches rose diagrams. This orientation corresponds to the trenches with evidence of recent activity.

# ENGINEERING GEOLOGY

## GEOLOGICAL STRENGTH INDEX (GSI)

The GSI was developed by Hoek and Brown (1997) as a quantitative way of relating field observations to the rock mass quality. It is based on the structure conditions (e.g., number of joints, joint density, bedding, shearing) and surface/weathering conditions observed in a homogeneous rock mass. The distribution of GSI estimates obtained at the Aishihik River landslide is shown in Figure 9. The average GSI value for both sidescarps was approximately 50-60. This corresponds to a blocky rock mass (i.e., three discontinuity sets) and fair surface conditions. The average GSI value for the backscarp of the slope failure was approximately 30 to 40. This indicates a very blocky rock mass (angular blocks due to the intersection of four discontinuity sets or more) with poor surface conditions.

## SCHMIDT HAMMER

The Schmidt Hammer is a non-destructive field test originally developed to test concrete hardness and first applied in rock engineering by Deere and Miller (1966). The average rebound values (R) can be correlated to the unconfined compressive strength (UCS) of the intact rock. Empirical relations between R and the UCS are specific to the rock lithology and weathering conditions (Dincer et al., 2004). The analysis in this study is conducted as a function of R, because empirical relations between R and UCS have not been derived for gneissic rock. Figure 10 illustrates the average rebound values obtained. The average rebound value calculated at each station ranged from 24 to 42. Four of the five average rebound values

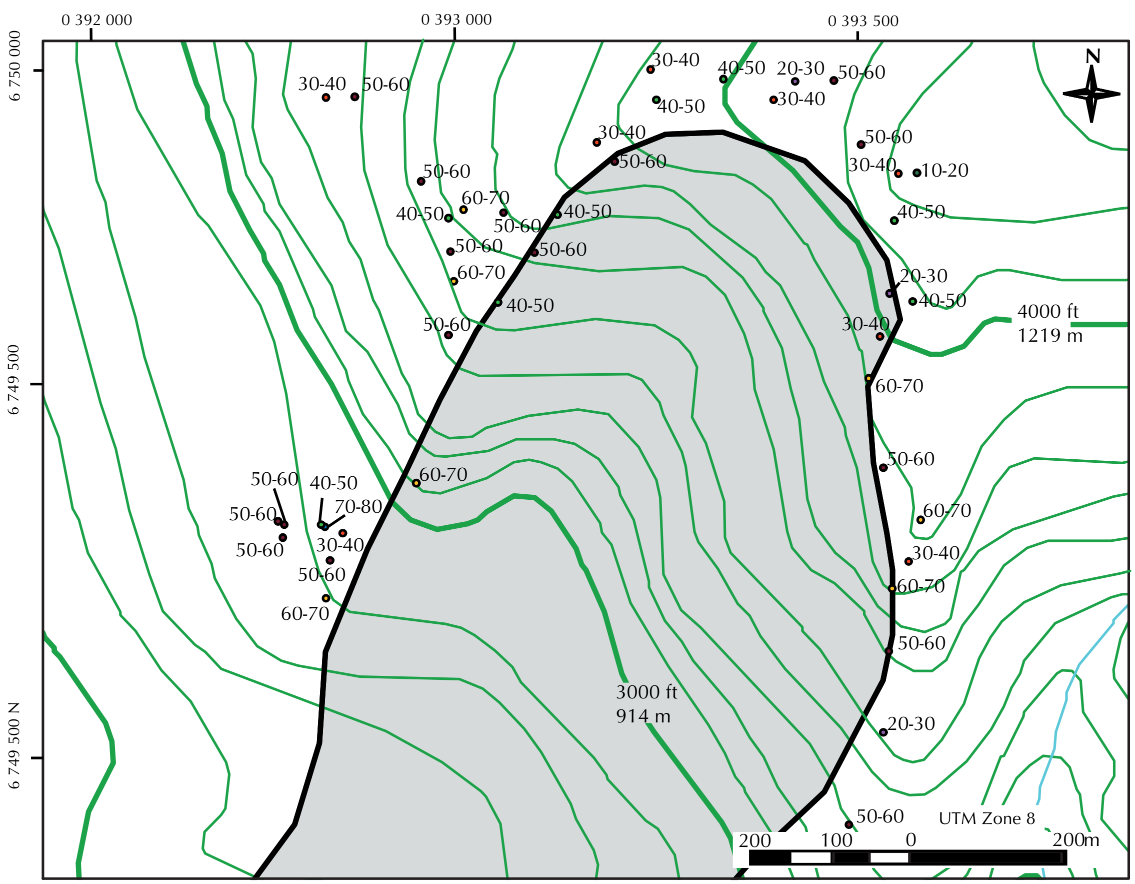


*Figure 9.* *GSI values recorded at the Aishihik River landslide.*

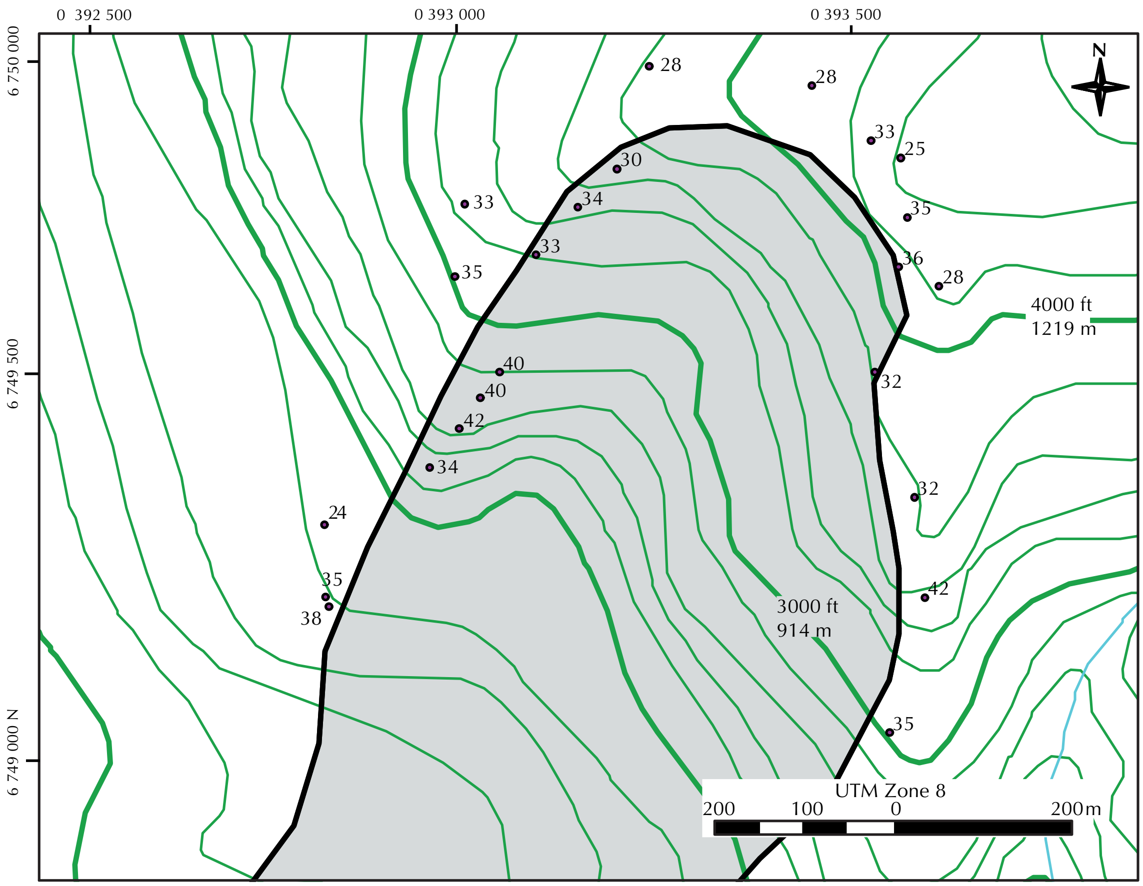


*Figure 10.* *Average Schmidt Hammer rebound number values obtained at the Aishihik River landslide.*

that were below thirty were recorded in the backscarp area. The lower rebound values from the headscarp area of the Aishihik River landslide correlate with the lower rock mass quality (GSI values).

## POINT LOAD TESTS

Point load tests were used to test the strength of rock samples collected at different locations around the slope failure. Tests were done according to the ISRM standard for irregular blocks (ISRM, 1985). Table 1 summarizes the point load index and corresponding uniaxial compressive strength (UCS) estimates obtained for the different lithologies. There was minimal variation in point load index between gneissic rocks that were tested perpendicular ($Is50_{perpendicular}$) and the samples tested parallel to the mineral foliation($Is50_{parallel}$). A point load anisotropy index ($Is50_{perpendicular}/Is50_{parallel}$) of 1.09 was calculated. The intact gneissic material is therefore considered to have isotropic strength characteristics. Point load index values obtained for the gneissic rocks correspond to values reported by Kulhawy (1975). The

*Table 1.* *Average point load index values and uniaxial compressive strength estimates obtained for the lithologies present at the Aishihik River landslide.*

| Lithology | point load index Is50 (MPa) | uniaxial compressive strength (MPa) | number of samples tested | number of tests performed |
|---|---|---|---|---|
| fresh grey intrusive | 13.3 | 293 | 4 | 7 |
| slightly ($W_1$) weathered intermediate intrusive | 2.1 | 46 | 1 | 2 |
| gneissic material parallel to foliation | 5.4 | 119 | 5 | 9 |
| gneissic material perpendicular to foliation | 5.9 | 130 | 4 | 9 |
| slightly ($W_1$) weathered fault material | 0.72 | 16 | 3 | 3 |

weathered materials had significantly lower point load index values (Table 1). The weathered samples were collected in zones that contained tectonic structures and their low point load index values could also be due to strength degradation related to tectonic damage of the rock mass. Results from point load tests on grey sills in the area demonstrate that these rocks have point load index values that are more than twice than those of the gneissic rocks.

# DISCUSSION

## TECTONIC DAMAGE

The influence of tectonic structures on slope stability was previously investigated in the southwestern Yukon by Everard (1994). An inventory of landslides and bedrock lineaments was derived from air photographs for the Kluane Lake, Mt. St. Elias, and the western half of the Dezadeash map areas. Bedrock lineaments were interpreted to represent the surface expression of faults by Everard (1994). The spatial distribution of landslides in southwestern Yukon is related to the presence of faults. Lithology and clusters of low-level earthquakes were also found to influence the spatial distribution of slope failures (Everard, 1994). Vanicek and Nagy (1981) reported that the highest 'present day' vertical crustal movement in Canada (24 mm/yr) was occurring in the southwestern Yukon at that time. This rate of uplift correlates to the 237 m of isostatic rebound in the Aishihik map area since deglaciation (Hughes, 1990). This large rebound and/or tectonic uplift rate is the principle cause of earthquakes and subsequent slope instability in southwestern Yukon (Clague, 1981).

The present study documents the tectonic structures in the region of the Aishihik River landslide, measures their effects on rock mass quality, and thereby provides an assessment of the implications for rock slope stability. Badger (2002) investigated fracturing related to anticlines and its influence on slope stability in a study of five sites in Washington State. Conceptual models suggest that when the fold-axis trend is parallel to the slope aspect but behind the slope crest, the slope would be predisposed to planar failure along shear fractures with tensile fractures acting as rear and lateral-release surfaces (Fig. 6). In the case of the Aishihik River landslide, the development of lateral-release surfaces would also be facilitated by faults perpendicular to the headscarp. The lower GSI, Schmidt Hammer rebound values, closer discontinuity spacing and complex discontinuity pattern collectively suggest that the headscarp area of the Aishihik River landslide is composed of a more damaged rock mass than the sidescarps. This lower rock mass quality facilitated the development of rear-release surfaces. The undercutting and subsequent debuttressing of the slope by glaciers during the last glaciation may have triggered the prehistoric Aishihik River landslide.

## FAILURE MECHANISMS

A kinematic analysis (Richards et al., 1978) that considers sliding, toppling and wedge failure mechanisms was performed (Fig. 11) to evaluate the model presented in Figure 6. The kinematic analysis was performed for two angles of friction (20° and 30°). The zone where each failure mechanism was kinematically feasible was delineated by a bold outline in each stereonet. Since the slope angle and discontinuity set III dip at ~30° the kinematic analysis performed for a friction angle of 30° suggests marginally stable conditions. The kinematic analysis performed using a friction angle of 20° suggests that sliding, toppling and wedge failures are all feasible failure mechanisms. Sliding and toppling failure mechanisms as represented in the conceptual model in Figure 6 would therefore only be kinematically feasible if the friction angle was below 30°. The shorelines deposited onto, and eroded into, the debris deposit suggest that the valley was still occupied by glacial lake Champagne when the slope failure occurred. The presence of water in the lower section of the slope could have reduced the effective friction angle along the discontinuities to the 20° value considered in the kinematic analysis.

Caution must be exerted when basic kinematic analysis techniques originally applied at the road-cut scale are to be applied to the mountain scale. Scale effects on the failure mechanism have been documented in physical and numerical models (Bandis and Barton, 1980; Hencher et al., 1996; Bhasin and Hoeg, 1998). Numerical and physical models suggest that rotation has a more important role in the failure mechanism of a region composed of a large number of blocks than the same region composed of fewer blocks (Bhasin and Hoeg, 1998). The number and size of blocks can be estimated during field investigation of rock slope by the spacing and persistence of discontinuities. For example, large rock slides in the Canadian Cordillera suggest that either wide spacing or a poor persistence of the subvertical discontinuity combined with a higher persistence of the

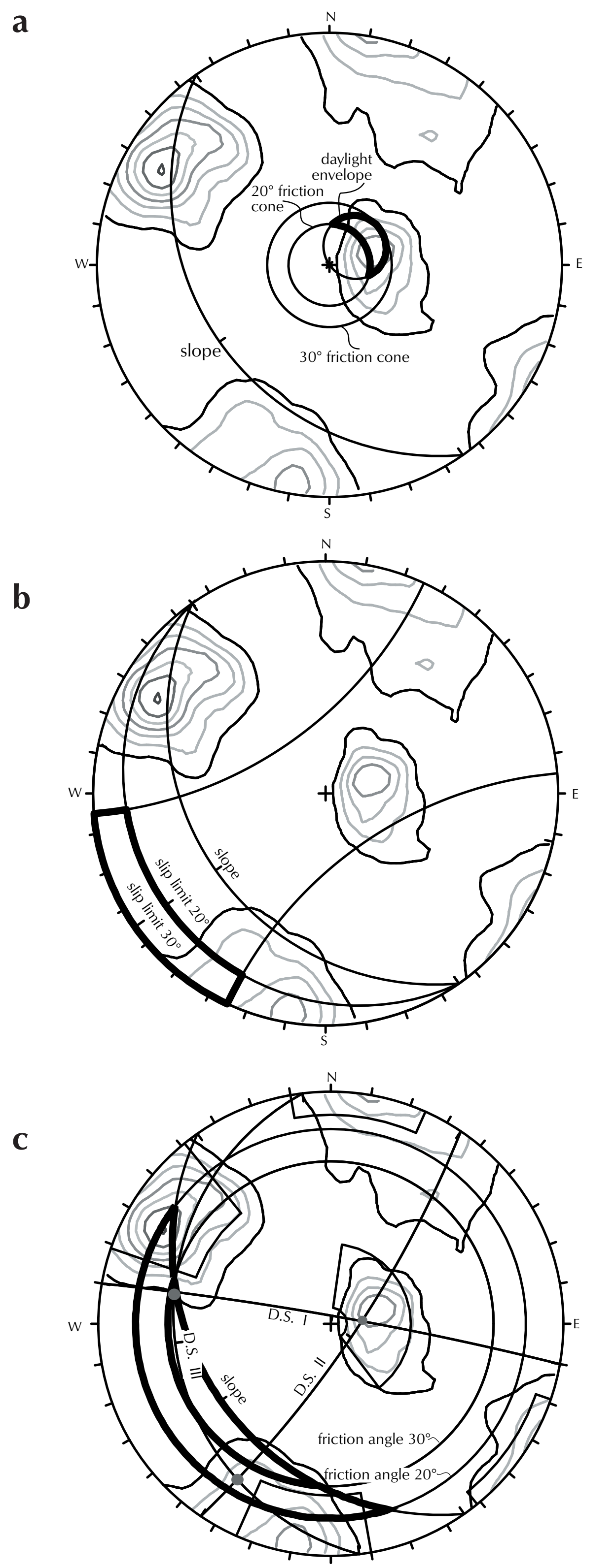


***Figure 11.** Kinematic analysis of the discontinuity sets recorded at the Aishihik River landslide. Analysis for **(a)** sliding, **(b)** toppling and **(c)** wedge failure mechanism.*

diagonal discontinuity was present. One of the largest rock slides in Canada, near Avalanche Lake (200 $mm^3$) in the Northwest Territories, was described as a slope failure along a 150-m-thick massive carbonate bed (Eisbacher, 1979; Evans et al., 1994). The moderate to wide spacing and low to medium persistence of all three discontinuity sets present at the Aishihik River landslide create a blocky rock mass (Fig. 12) which is unlikely to fail as a simple translational planar event. Numerical simulation will be used to further investigate possible failure mechanisms.

## PRESENT STABILITY CONDITIONS

Observations made during fieldwork and a review of the air photographs provide a preliminary assessment of the current stability of the rock slope adjacent to the slope failure. Recent movement at the study site is indicated in the headscarp area by exposed soil and White River Ash in trenches, and disturbance to the vegetation (Huscroft et al., 2004). Both sidescarps are composed of a series of down-dropped blocks. The headscarp of the Aishihik River landslide extends beyond the western limit of failed material. Active block toppling and rock fall zones are present on the western sidescarp.

Such signs of ongoing instability over much of a prehistoric failure area and adjacent area along the valley side have important implications for hazard assessment. Further study and a hazard assessment should precede any development of the area proximal to the Aishihik River landslide. This study should investigate the rate of movement on the trenches and tension cracks and include a runout analysis. Runout analyses investigate how far a landslide will likely travel. They are important in evaluating which infrastructures are at risk. Field observations acquired during this project suggest that there is the potential for a future failure of a similar


***Figure 12.** Blocky nature of the southwestern ridge. View looking northeast.*

volume to the prehistoric Aishihik River landslide. A travel distance similar to that of the previous slope failure should be considered a minimum.

## CONCLUSIONS

The origin of the three dominant discontinuity sets present at this landslide are explained by a simple fracture model related to the formation of the regional antiform. The structural domains, discontinuity spacing, Geological Strength Index and average Schmidt Hammer measurements suggest that the headscarp region of the slope failure comprises lower quality rock than the regions on either side. Analysis of known faults, bedrock lineaments, discontinuities, tension cracks and trenches reveals a preferential northeast orientation that corresponds to the orientation of the failed material and transport direction. Pre-existing tectonic conditions have played an important role in reducing the rock mass quality and strength in the headscarp of the Aishihik River landslide, thereby facilitating the development of a rear-release surface. Point load tests suggest that the rock mass has a nearly isotropic intact rock strength. Geomorphic evidence of present-day slope instability at the Aishihik River landslide was observed during this project and by previous workers, and has implications for future development in the area.

## ACKNOWLEDGEMENTS

The authors would like to thank B. Ward for his critical review of the manuscript. We would also like to thank J.E. Mezger for access to his field notes and discussions on the regional structural geology, J. Bond for discussions on the glacial lakes in southern Yukon and D. Froese for discussions on the tephra found in the southwestern Yukon. Funding for this project was provided by an NSERC Discovery grant to D. Stead and an NSTP grant to M.-A. Brideau.

## REFERENCES

Badger, T.C., 2002. Fracturing within anticlines and its kinematic control on slope stability. Environmental and Engineering Geoscience, vol. VIII, no. 1, p. 19-33.

Bandis, S.C. and Barton, N.R., 1980. Some effects of scale on the shear strength of joints. International Journal of Rock Mechanics, Mining Sciences and Geomechanic Abstract, vol. 17, p. 69-73.

Barnes, S.D., 1997. The sedimentology and paleo–geography of glacial lake Champagne, southern Yukon Territory. Unpublished M.Sc. thesis, Carleton University, Ottawa, Ontario, 109 p.

Barnes, S.D., 2000. The paleogeography of glacial lake Champagne, southern Yukon: Implications for the last deglaciation. 30th International Arctic Workshop, Program and Abstracts, 2000, Institute of Arctic and Alpine Research, University of Colorado, Boulder, Colorado, p. 17-19.

Bhasin, R. and Hoeg, K., 1998. Numerical modelling of block size effects and influence of joint properties in multiply jointed rock. Tunneling and Underground Space Technology, vol. 13, no. 2, p. 181-188.

Clague, J.J., Evans, S.G., Rampton, V.N., and Woodsworth, G.J., 1995. Improved age estimates for the White River and Bridge River tephras, Western Canada. Canadian Journal of Earth Sciences, vol. 32, no. 8, p. 1172-1179.

Clague, J.J., 1981. Landslides at the south end of Kluane Lake, Yukon Territory. Canadian Journal of Earth Sciences, vol. 18, p. 959-971.

Couture, R. and Evans, S.G., 2000. The East Gate Landslide, Beaver Valley, Glacier National Park, Columbia Mountains, British Columbia. Geological Survey of Canada, Open File 3877, p. 1-26.

Davis G.H. and Reynolds, S.J., 1996. Structural Geology of Rocks and Regions, 2nd Edition. Wiley Publishing, New York, New York, 776 p.

Deere, D.U. and Miller, R.P., 1966. Engineering classification and index properties for intact rock, Report AFWL-TR-65-116, Air Force Weapons Laboratory, 300 p.

Dincer, I., Acar, A., Cobano, I. and Uras, Y., 2004. Correlation between Schmidt hardness, uniaxial compressive strength and Young's modulus for andesites, basalts and tuffs. Bulletin of Engineering Geology and the Environment, vol. 63, no. 2, p. 141-148.

Eisbacher, G.H., 1979. Cliff collapse and rock avalanches (sturzstroms) in the Mackenzie Mountains, Northwestern Canada. Canadian Geotechnical Journal, vol. 16, p. 309-334.

Evans, S.G., Hungr, O. and Enegren, E.G., 1994. The Avalanche Lake rock avalanche, Mackenzie Mountains, Northwest Territories, Canada: Description, dating, and dynamics. Canadian Geotechnical Journal, vol. 31, p. 749-768.

Everard, K.A., 1994. Regional characterization of large landslides in southwest Yukon, with emphasis on the role of neotectonics. Unpublished M.A.Sc., University of British Columbia, Vancouver, British Columbia, 165 p.

Gordey, S.P. and Makepeace, A.J., (compilers), 2000. Yukon Digital Geology. Geological Survey of Canada, Open File D3826 or Exploration and Geological Services Division, Yukon Region, Indian and Northern Affairs Canada, Open File 1999-1(D), 2 CD-ROMs.

Hencher, S.R., Liao, Q-H. and Monaghan, B.G., 1996. Modelling slope behaviour for open-pits. Transactions of the Institution of Mining and Metallurgy Section A-Mining Industry, vol. 105, p. A37-A47.

Hoek, E. and Brown, E.T., 1997. Practical estimates of rock mass strength. International Journal of Rock Mechanics and Mining Sciences, vol. 34, no. 8, p. 1165-1186.

Hughes, O.L., 1990. Surficial geology and geomorphology, Aishihik Lake, Yukon Territory. Geological Survey of Canada, Paper 87-29, 23 p.

Hughes, O.L., Rutter, N.W. and Clague, J.J., 1989. Yukon Territory (Quaternary stratigraphy and history, Cordilleran Ice Sheet). *In:* Chapter 1 of Quaternary Geology of Canada and Greenland Volume, R.J. Fulton (ed.); Quaternary; Geological Survey of Canada; also Geological Society of America, The Geology of North America vol. K-1, p. 58-62.

Huscroft, C., Lipovsky, P. and Bond, J., 2004. A regional characterization of landslides in the Alaska Highway Corridor, Yukon. Yukon Geological Survey Open File 2004-18, 65 p, includes CD-ROM.

ISRM, 1978. Suggested methods for the quantitative description of discontinuities in rock masses. International Journal of Rock Mechanics and Mining Sciences and Geomechanics Abstracts, vol. 15 p. 319-368.

ISRM, 1985. Suggested method for determining point load strength. International Journal of Rock Mechanics and Mining Sciences and Geomechanics Abstracts, vol. 22, no. 2, p. 51-60.

Kindle, E.D., 1952. Dezadeash map-area, Yukon Territory. Memoir 268, Geological Survey of Canada, 68 p.

Kulhawy, F.H., 1975. Stress deformation properties of rock and rock discontinuities. Engineering Geology, vol. 9, p. 327-350.

Lerbekmo, J.F. and Campbell, F.A., 1969. Distribution, composition, and source of the White River Ash, Yukon Territory. Canadian Journal of Earth Sciences, vol. 6, no. 1, p. 109-116.

Mathews, W.H. and McTaggart, K.C., 1969. The Hope landslide, British Columbia. In The Geological Association of Canada, vol. 20, p. 65-75.

Mezger, J.E., 1997. Tectonometamorphic evolution of the Kluane metamorphic assemblage, SW Yukon: Evidence for Late Cretaceous eastward subduction of oceanic crust underneath North America. Unpublished Ph.D. Thesis, University of Alberta, Edmonton, Alberta, 324 p.

Mezger, J.E., 2000. 'Alpine-type' ultramafic rocks of the Kluane metamorphic assemblage, southwest Yukon: Oceanic crust fragments of a late Mesozoic back-arc basin along the northern Coast Belt. *In:* Yukon Exploration and Geology 1999, D.S. Emond and L.H. Weston (eds.), Exploration and Geological Services Division, Yukon Region, Indian and Northern Affairs Canada, p. 127-138.

Mezger, J.E., 2003. Geology of the Dezadeash Range and adjacent northern Coast Mountains (115A), southwestern Yukon: Re-examination of a terrane boundary. *In:* Yukon Exploration and Geology 2002, D.S. Emond and L.L. Lewis (eds.), Exploration and Geological Services Division, Yukon Region, Indian and Northern Affairs Canada, p. 149-163.

Muller, J.E., 1967. Kluane Lake map-area, Yukon Territory (115G, 115F E1/2). Geological Survey of Canada Memoir 340, 137 p.

Price, N.J. and Cosgrove, J.W., 1990. Analysis of geological structures. Cambridge University Press, Cambridge, UK, 502 p.

Rampton, V.N. and Paradis, S., 1981. Surficial geology and geomorphology Taye Lake, YT. Geological Survey of Canada, Map 14-1981, 1:100 000 scale

Richards, L.R., Leg, G.M.M. and Whittle, R.A., 1978. Appraisal of stability conditions in rock slopes. *In:* Foundation Engineering in Difficult Ground, F.G. Bell (ed.). Newnes-Butterworth, London, UK, p. 449-512.

Twiss, R.J. and Moore, E.M., 1992. Structural geology. W.H. Freeman and Company, New York, New York, 532 p.

Vanicek, P. and Nagy, D., 1981. On the compilation of the map of contempory vertical crustal movements in Canada. Techonophysics, vol. 71, p. 75-86.